Controllable red and blue shifting of InGaAsP quantum well bandgap energy for photonic device integration

2015 Mater. Res. Express 2 086302

(http://iopscience.iop.org/2053-1591/2/8/086302)

Materials Research Express

PAPER

RECEIVED
10 June 2015

REVISED
20 July 2015

ACCEPTED FOR PUBLICATION
31 July 2015

PUBLISHED
19 August 2015

Controllable red and blue shifting of InGaAsP quantum well bandgap energy for photonic device integration

P Aleahmad, S Bakhshi, D Christodoulides and P LiKamWa

CREOL, The College of Optics & Photonics, University of Central Florida, Orlando, FL 32816, USA

E-mail: parinaz.aleahmad@creol.ucf.edu

Keywords: bandgap tuning, quantum wells, photonic device integration

Abstract

We demonstrate bandgap tuning of InGaAsP multiple quantum well structures by utilizing an impurity-free vacancy diffusion technique. Substantial modification of the bandgap energy toward the red and blue parts of the spectrum has been observed using $SiO_2/SiO_yN_x/SiN_x$ capping layers and by controlling the associated oxygen and nitrogen content. The resulting degree of tuning, up to 120 nm red shift and 140 nm blue shift of the band-to-band wavelength emission, has been studied using room-temperature photoluminescence, in agreement with the emission spectra obtained from semiconductor optical amplifier waveguide strips.

Selective area bandgap tuning of multiple quantum well structures (MQWs) has been an ongoing task in optoelectronic device fabrication in the past few decades [1–17]. This matter is of particular importance in the fabrication of high-performance laser diodes and photonic integrated circuits [18–22]. Among the variety of available techniques a great deal of attention has been focused on induced disordering of MQWs by impurity-free vacancy diffusion (IFVD), due to its inherent spatial selectivity between adjacent regions and its ability to conserve the electrical properties of the disordered and non-disordered sections alike. IFVD techniques, however, rely on the application of a capping layer, usually SiO_2/SiN_x, which promotes the out-diffusion of Ga from the top surface of the wafer into the dielectric film, thus leaving vacancies in the group III sublattice during a high-temperature rapid thermal annealing. While the relative simplicity of IFVD is an asset, the degree of intermixing that can be achieved through this technique is significantly susceptible to the film properties, the specific structure of MQW, the annealing conditions and even the duration of surface exposure to radio-frequency plasma during reactive ion etching [15, 17].

In the intermixing of InGaAsP MQWs, a SiO_2 cap is usually employed to achieve considerable blue shift to the bandgap transition wavelength of up to 100 nm [10, 11, 14], while a SiN_x cap behaves as an inhibitor to the intermixing process. On rare occasions, the MQW region covered by the SiN_x cap undergoes a very slight bandgap change after the rapid thermal annealing [10, 11, 14]. In this work we demonstrate a significant range in the degree of bandgap modification (up to 140 nm in wavelength shift towards the blue wavelengths and 120 nm towards the red) by manipulating the chemical compositions of the SiO_yN_x and SiN_x films. These bandgap tunings have been determined by measuring the room-temperature photoluminescence spectra of the disordered MQW samples. The reduction in the bandgap energy is also corroborated by measuring the emission spectra of several semiconductor optical amplifier (SOA) waveguide strips, fabricated on the MQW wafer that was covered by SiN_x during the rapid thermal annealing.

In this study we have examined two different MQW wafers (A and B). Both structures involve six InGaAsP quantum wells grown by metal organic chemical vapor deposition (MOCVD) at a commercial semiconductor foundry. Each p–i–n structure is grown epitaxially on a Si-doped InP substrate with a 70 nm thick undoped InP buffer at the p–i interface. The active region of wafer A consists of six undoped InGaAsP ($\lambda_g = 1.56\ \mu$m) quantum wells each 10 nm thick sandwiched between five undoped layers of 15 nm thick InGaAsP ($\lambda_g = 1.13\ \mu$m) barriers while that of wafer B consists of six undoped InGaAsP ($\lambda_g = 1.59\ \mu$m) quantum wells each 8 nm thick sandwiched between five undoped layers of 15 nm thick InGaAsP ($\lambda_g = 1.13\ \mu$m) barriers, where λ_g is the bandgap wavelength. A schematic cross-sectional view of the wafer design is shown in figure 1.

InGaAs p-type	150 nm
InP p-type (Zn dopped)	1550 nm
InGaAsP U/D	70 nm
5 × InGaAsP (15nm)/6 × InGaAsP(10nm)	
InGaAsP U/D	70 nm
InP n-type (Si dopped)	2500 nm
InGaAs n-type (Si dopped)	50 nm
InP Substrate (Si dopped)	

Figure 1. Schematic cross-sectional view of MQW design A grown by MOCVD.

The samples used in this study were ultrasonically cleaned with acetone to remove debris and organic residue from the top layer, followed by rinsing with isopropyl alcohol and deionized water. The samples were then immersed in buffered oxide etch to remove any native oxide from the surface. In order to study the dependence of bandgap tuning of the MQWs on the different dielectric capping layers, a number of samples are prepared with a variety of SiO_2, SiN_x and SiO_yN_x films grown by plasma-enhanced chemical vapor deposition (PECVD). After each individual sample was coated with a film of SiN_x or SiO_yN_x, the film was removed from half of the surface using a photoresist mask and reactive ion etching. After removal of the photoresist, a final layer of SiO_2 is grown by PECVD to cover everything. Consequently all the samples contain two sections: an area that is covered by a single layer of SiO_2 and the remaining area that is covered with either SiN_x or SiO_yN_x followed by an overlayer of SiO_2. The latter is expected to inhibit intermixing. To formulate SiO_yN_x films with various compositions, the ratio of N_2O to NH_3 used in the PECVD process is varied from five to one in small steps. Evidently a higher ratio of N_2O/NH_3 results in a SiO_yN_x film with a larger oxygen content and hence the film has a lower refractive index. On the other hand, the SiN_x film is grown in the absence of any N_2O gas, and the composition is controlled by varying the ratio of SiH_4 to NH_3 during the PECVD process. In this case, higher SiH_4 to NH_3 ratios lead to Si-rich films that have higher refractive indices. Therefore the refractive index of the film was used as a measure of the composition of SiN_x or SiO_yN_x. Our PECVD machine utilizes a 2% silane gas (SiH_4) pre-diluted with nitrogen gas and the SiN_x films are usually under high tensile stress. By adding N_2 and He to the growth recipes, the tensile or compressive behavior of the SiN_x films can be controlled. However, it was found that there was always some residual stress in the films, and the only effective way to prevent film cracking during high-temperature anneals was to limit the thickness of the SiN_x/SiO_yN_x films to less than 50 nm. In this study, the thickness of the SiN_x/SiO_yN_x films was kept at 30 nm as a good compromise between repeatability and film robustness to high-temperature anneals. On the other hand, the thickness of the SiO_2 film that is expected to promote the intermixing is kept at 200 nm for all the samples. Each sample was treated individually in a rapid thermal annealer (RTA) for 30 s at 800 °C. During the RTA process, the MQW samples were sandwiched between two GaAs wafers to maintain an As overpressure and minimize the outgassing of As from the samples. Figure 2 outlines the characteristic changes of the photoluminescence (PL) spectra measured at room temperature for the samples of MQW wafer A that were covered with different film compositions and annealed at 800 °C for 30 s. The absolute values of the shift in PL peak from that of the as-grown sample are plotted in figure 2 as a function of the refractive index of the covering film. The down-pointing and up-pointing triangles correspond to samples covered with SiO_yN_x and SiN_x respectively. Overall, the shift of the PL peak that was obtained using the different film compositions is in the range from −140 nm to +120 nm. The results shown in figure 2 indicate that the SiO_yN_x films that were grown using PECVD processes containing N_2O in the gas mixture tend to result in blue shifts of the PL peak, similar to SiO_2 films, but to varying degrees depending on the ratio of the NH_3 to N_2O mixture. Larger ratios of NH_3/N_2O produce SiO_yN_x films that contain larger x/y ratios with correspondingly higher refractive indices, and tend to shift the PL to a longer wavelength. In the absence of N_2O during the PECVD process, the SiN_x films lead to red-shifting of the PL peak. However, it was observed that

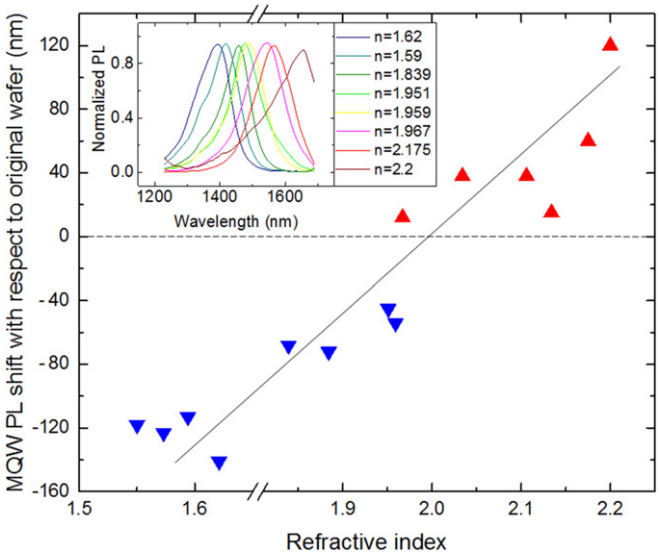

Figure 2. Absolute value of the PL shift measured from RTA treated samples capped with different dielectric films, with respect to the refractive index of the film. The blue shift associated with SiON films for different ratios of NH3/N2O, while the red shift refers Si-rich compositions. The inset shows the absolute PL spectrum for selected data points.

Table 1. Recipes for SiN/SiO_yN_x film composition ordered by their refractive index.

	Power	Temp.	SiH_4	NH_3	N_2O	N_2	He	Refractive
	(W)	(°C)	(sccm)	(sccm)	(sccm)	(sccm)	(sccm)	index
1	150	300	200	4	20	800	0	1.55
2	100	250	200	10	35	600	0	1.573
3	100	250	200	10	29	600	0	1.594
4	150	300	180	3.5	10	800	0	1.621
5	150	300	180	3.5	5	800	0	1.839
6	100	250	180	4.2	0	200	219	1.884
7	150	300	180	4	0	0	450	1.951
8	150	300	200	4	4	800	0	1.959
9	100	250	240	4	0	200	219	1.967
10	150	300	180	4.2	0	200	219	2.034
11	150	300	180	3.75	0	200	219	2.106
12	150	300	200	4	0	800	0	2.134
13	150	300	220	4	0	200	219	2.175
14	150	300	200	3.5	0	800	0	2.2

the degree of the PL peak shift could be controlled by the ratio of SiH_4 to NH_3 gases during the PECVD growth of the capping film. A larger ratio of SiH_4/NH_3 leads to a film of higher refractive index, which is consistent with a Si-rich film that results in a MQW disordering with more bandgap narrowing. The SiO_2-covered sections of all these samples exhibited a blue shift of 140 nm in the PL peak. Table 1 shows a summary of the pertinent parameters that were employed in the PECVD growth of the SiO_yN_x/SiN_x films.

Noting the compelling nature of this new observation of significant bandgap narrowing caused by selective area intermixing of InGaAsP MQWs, we decided to verify this technique of bandgap tuning using SiN_x films of varying Si compositions on the MQW wafer B. To reduce any other unintended influences, in the growth of the SiN_x films the SiH_4, He and N_2 mass flow rates as well as the plasma rf power and the substrate temperature were all kept constant while changing the NH_3 flow for all different recipes. Figure 3 shows the photoluminescence spectrum shift of the MQW structure toward red for dielectric capping films with varying Si concentrations, treated with RTA. The results clearly show a red shifting of the PL peak emission for Si-rich compositions of SiN_x with the largest shift occurring when the ratio of SiH_4 to NH_3 is highest during the PECVD process.

In order to eliminate the possibility of the red-shifted PL spectra being caused by an unintended embedded layer in the semiconductor wafer, the cladding coating of the wafer shown in figure 1 has been removed layer by layer and the photoluminescence spectrum of the wafer measured separately each time. As a result no change was revealed in the PL spectrum of a red-shifted sample. To investigate this issue further, the

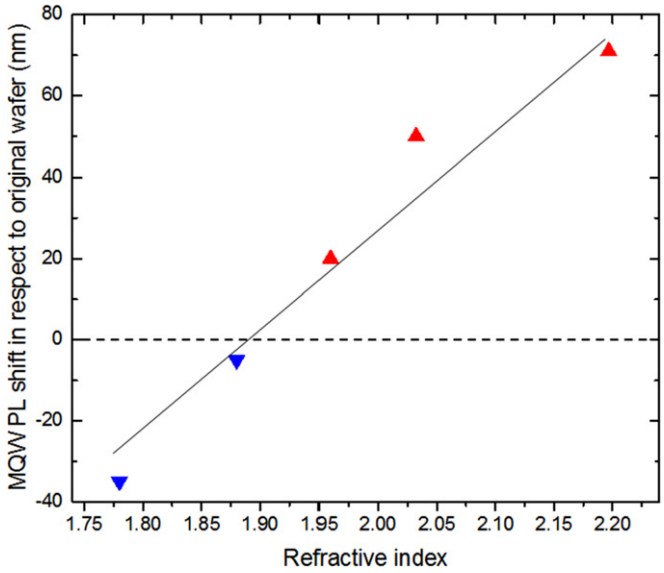

Figure 3. Absolute value of the PL shift with respect to the refractive index of SiN_x capping films.

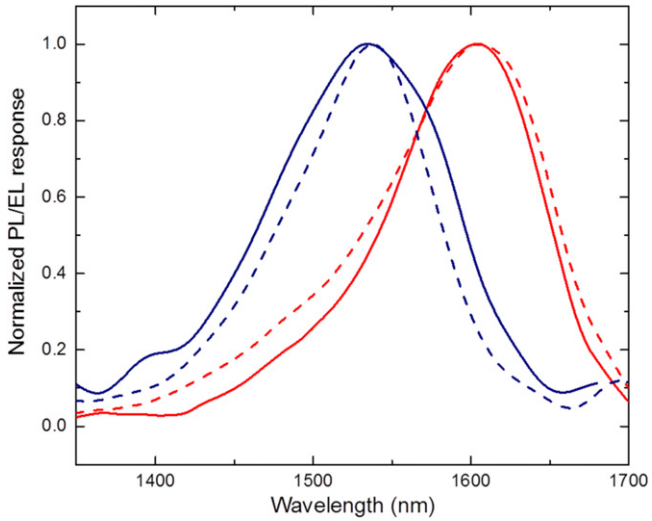

Figure 4. The electroluminescence and photoluminescence response of a red-shifted sample and a blue-shifted sample. The solid line indicates the PL while the dashed line represents the EL spectrum.

electroluminescence spectrum of both red- and blue-shifted samples was obtained (figure 4). This measurement was performed utilizing a semiconductor optical amplifier (SOA) fabricated on a waveguide strip.

In conclusion, we have presented a thorough study of broad bandgap tuning for InGaAs(P)/InP-based multistructure quantum wells, up to 140 nm toward the blue and 120 nm toward the red parts of the spectrum, employing SiO_yN_x/SiN_x PECVD-grown films. We examined new techniques to achieve absolute red shifts of the bandgap with selectivity over a broad spectrum. This process is controlled by the Si concentration in the film compositions. These results could potentially be useful in the fabrication of high-performance laser diodes and photonic integrated circuits.

Acknowledgments

This work was supported by NSF (Grant No. ECCS-1128520) and AFOSR (Grants No. FA9550-12-1-0148 and No. FA9550-14-1-0037).

References

[1] Rao S, Gillin W and Homewood K 1994 Interdiffusion of the group-III sublattice in In-Ga-As-P/In-Ga-As-P and In-Ga-As/In-Ga-As heterostructures *Phys. Rev.* B **50** 8071–3

[2] Rao E V K *et al* 1995 New encapsulant source for III–V quantum well disordering *Appl. Phys. Lett.* **66** 472

[3] Pepin A *et al* 1997 Evidence of stress dependence in SiO_2/Si_3N_4 encapsulation-based layer disordering of GaAs/AlGaAs quantum well heterostructures *J. Vac. Sci. Technol.* B **15** 142–53

[4] Choi J *et al* 1998 Dependence of dielectric-cap quantum-well disordering of GaAs-AlGaAs quantum-well structure on the hydrogen content in SiN_x capping layer *IEEE J. Sel. Top. Quantum Electron.* **4** 624–8

[5] Kowalski O P *et al* 1998 A universal damage induced technique for quantum well intermixing *Appl. Phys. Lett.* **72** 581

[6] Sang Kee S *et al* 1998 Area selectivity of InGaAsP-InP multiquantum-well intermixing by impurity-free vacancy diffusion *IEEE J. Sel. Top. Quantum Electron.* **4** 619–23

[7] Helmy A S *et al* 1999 Control of silica cap properties by oxygen plasma treatment for single-cap selective impurity free vacancy disordering *Appl. Phys. Lett.* **74** 732–4

[8] Liu X F *et al* 2000 Control of multiple bandgap shifts in InGaAs-AlInGaAs multiple-quantum-well material using different thicknesses of PECVD SiO_2 protection layers *IEEE Photonics Technol. Lett.* **12** 1141–3

[9] Lee A S W *et al* 2001 Enhanced band-gap blueshift due to group V intermixing in InGaAsP multiple quantum well laser structures induced by low temperature grown InP *Appl. Phys. Lett.* **78** 3199

[10] Teng J H *et al* 2002 Controlled group V intermixing in InGaAsP quantum well structures and its application to the fabrication of two section tunable lasers *J. Appl. Phys.* **92** 4330

[11] Choi W J *et al* 2004 Dependence of the intermixing in InGaAs/InGaAsP quantum well on capping layers *J. Korean Phys. Soc.* **45** 773–6

[12] Skogen E J *et al* 2005 Multiple-band-edge quantum-well intermixing in the InGaAs/InGaAsP/InGaP material system *Appl. Phys. Lett.* **86** 241117

[13] Helmy A S *et al* 2006 Spatially resolved photoluminescence and Raman spectroscopy of bandgap gratings fabricated in GaAs/AlAs superlattice waveguide using quantum well intermixing *J. Cryst. Growth* **288** 53–6

[14] Yu J S and Lee Y T 2007 Impurity-free vacancy diffusion of InGaAsP/InGaAsP multiple quantum well structures using SiH_4-dependent dielectric cappings *Japan. J. Appl. Phys.* **46** 6509–13

[15] May-Arrioja D A *et al* 2009 Intermixing of InP-based multiple quantum wells for integrated optoelectronic devices *Microelectron. J.* **40** 574–6

[16] McKerracher I *et al* 2012 Intermixing of InGaAs/GaAs quantum wells and quantum dots using sputter-deposited silicon oxynitride capping layers *J. Appl. Phys.* **112** 113511

[17] Bickel N and LikamWa P 2011 Enhanced control over selective-area intermixing of $In_{0.15}Ga_{0.85}As/GaAs$ quantum dots through post-growth exposure to radio-frequency plasma *Thin Solid Films* **519** 1955–9

[18] Yu S F and Li E H 1998 Semiconductor lasers using diffused quantum-well structures *IEEE J. Sel. Top. Quantum Electron.* **4** 723–35

[19] Kim C *et al* 2000 Ultrafast all-optical multiple quantum well integrated optic switch *Electron. Lett.* **36** 1929–30

[20] Choy W C H and Chan K S 2003 Theoretical analysis of diffused quantum-well lasers and optical amplifiers *IEEE J. Sel. Top. Quantum Electron.* **9** 698–707

[21] Taniguchi H *et al* 2007 25-W 915 nm lasers with window structure fabricated by impurity-free vacancy disordering (IFVD) *IEEE J. Sel. Top. Quantum Electron.* **13** 1176–9

[22] Zhao J *et al* 2012 Spatial control based quantum well intermixing in InP/InGaAsP structures using ICP *J. Semicond.* **33** 106001